Investigating a (Natural) Killer by Studying the Victims:

Searching for Mechanisms to Selectively Inhibit NK-cell Immunosuppressive Function to Improve Vaccine Responses

Andrew Cox[1,2], Alex Katko[3,4], Krishna Roskin[3,5], Stephen Waggoner[2,4,5]

[1]Division of Infectious Diseases, Cincinnati Children's Hospital Medical Center; [2]Center for Autoimmune Genomics and Etiology, Cincinnati Children's Hospital Medical Center; [3]Division of Immunobiology, Cincinnati Children's Hospital Medical Center; [4]Medical Scientist Training Program, University of Cincinnati College of Medicine; [5]Department of Pediatrics, University of Cincinnati College of Medicine

Cincinnati Children's® changing the outcome together

NK cells restrain vaccine responses

Decades of effort have yet to deliver an efficacious vaccine for pathogens such as HIV, despite major revelations about HIV antigens and development of new vaccine platforms (i.e. mRNA vaccines). Innovative outside-the-box approaches are needed to overcome immunological roadblocks to the success of past and current vaccine regimens. We discovered that natural killer (NK) cells are a potent obstacle to vaccine success through perforin-dependent suppression of activated CD4 T cell responses early after vaccination [1-3]. This killing reduces the quantity and quality of antibody responses. Yet, the features of NK cells that enable this activity or determine susceptibility of specific subsets of T cells remain ill-defined.

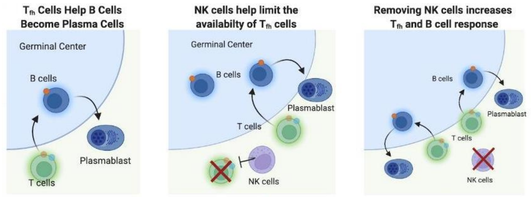

Figure 1. NK cells limit availability of T_{FH} which limits B cell responses.

NK cells limit T_{FH} responses and affinity maturation in a perforin dependent manner

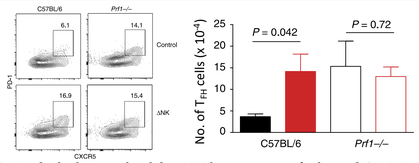

Figure 2. Perforin is required for NK immunoregulation of CD4 T cells. Groups of C57BL/6 or *Prf1*-/- mice were depleted of NK cells (ΔNK/red) or administered control antibody (Control/black) 1 day before infection with $5e^4$ PFU LCMV Armstrong. (**left**) Representative staining of T_{FH} markers CXCR5 and PD-1 on activated ($CD44^{hi}$) CD4 T cells in the spleen 5 days post infection. (**right**) Numbers of T_{FH} cells (PD-1^+ $CXCR5^+$ $CD44^{hi}$ $CD4^+$) in the spleen on day 5 post infection. (mean ± s.e.m.) ***Figure from reference 1.***

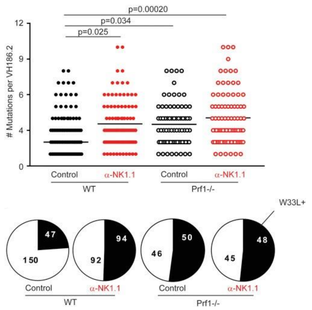

Figure 3. NK depletion increases the percentage of affinity maturing somatic hypermutated B cells. Number of mutations per sequenced heavy chain in control or NK-cell depleted WT or *Prf1*$^{-/-}$ mice on day 12 post-immunization with NP-KLH. Data were analyzed via Kruskal-Wallis with multiple testing correction Proportion of unique V_H186.2 sequences bearing the affinity conferring W33L mutation. ***Figure from reference 2.***

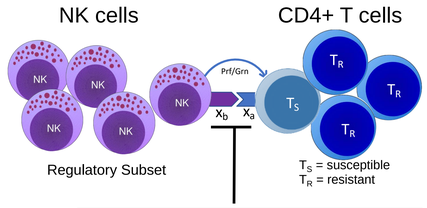

Block unknown receptor ligand interaction

Study Aim:

Discover the parameters that render CD4 T cells susceptible to NK cell mediated killing in the context of vaccination.

We leverage transgenic CD4 T cells to study early time points post infection.

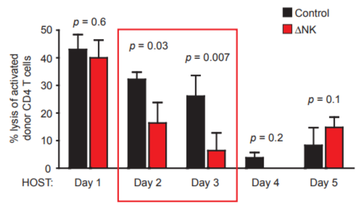

Figure 5. NK cell immunoregulation peaks 2 to 3 days post infection. In vivo cytotoxicity assay demonstrating in vivo loss of activated donor ($Ly5.1^+$) T cells from NK cell-depleted, LCMV infected mice 5 h after transfer into control or NK-depleted (ΔNK) $Ly5.2^+$ mice infected one to five days previously with medium dose LCMV, relative to cells transferred into uninfected host mice. (mean±s.e.m.) ***Figure from reference 3***.

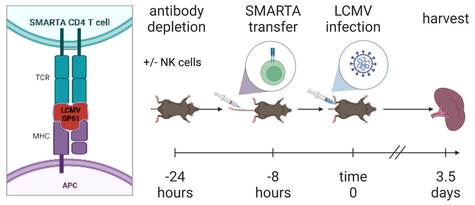

Figure 6. Experimental Design. 8–12-week-old C57BL/6 mice were treated with 25µg anti-NK1.1 or isotype control Ab. The next day 5 x 10^5 CD4 enriched splenocytes were transferred via retro-orbital injection from LCMV GP TCR transgenic SMARTA mice. Mice were later infected with $5e^4$ PFU LCMV Armstrong and harvested 3.5 days later.

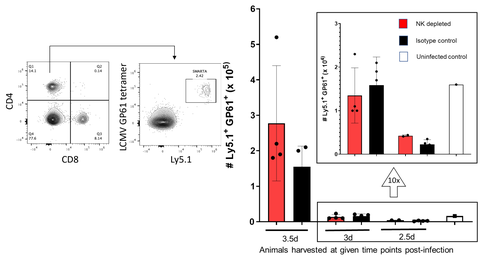

Figure 7. T cells do not start expanding until 72 hours post infection Representative staining of SMARTA markers Ly5.1 and LCMV GP61 Class II tetramer. Numbers of SMARTA in the spleen on day of harvest (mean±s.e.m.)

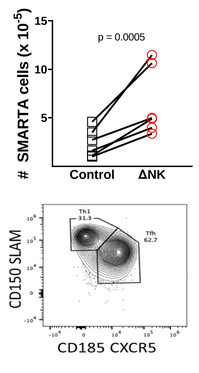

Figure 8. An increase in SMARTA with NK depletion is seen across multiple experiments. Groups of C57BL/6 mice (n=4 per group repeated 6 times) were treated as above and harvested at day 3.5 post-infection and the number of CD45.1 CD4 tetramer + CD4 T cells is shown.

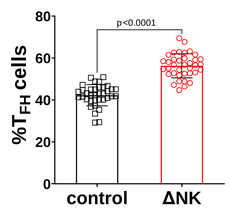

Figure 9. SMARTA display increased frequency of T_{FH} early after infection. Groups of C57BL/6 mice (n=4 per group repeated 6 times) were treated as above and harvested at day 3.5 post-infection. (left) Representative staining of T_{FH} gating ($SLAM^{lo}$ $CXCR5^{hi}$). (right) Percent of SMARTA that are T_{FH} ($SLAM^{lo}$ $CXCR5^{hi}$) (mean±s.e.m.)

Single Cell RNA sequencing reveals a candidate transcript *Cxcl10.*

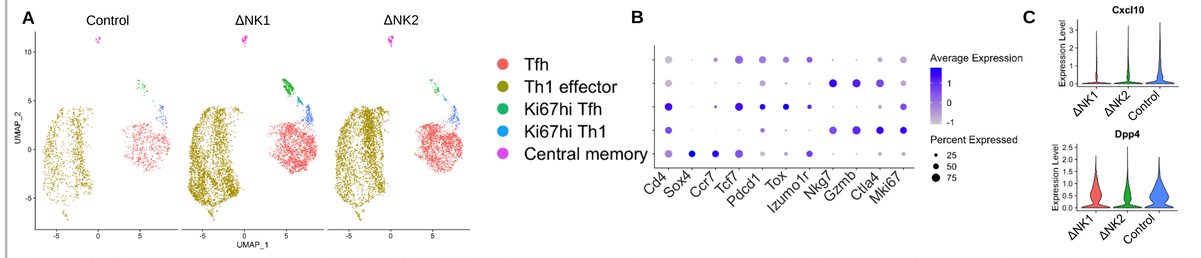

Figure 10. Single cell RNA sequencing identifies differentially expressed genes amongst the T_{FH} group. Cells were harvested as in Figure 3 enriched for CD4 T cells then sorted for live, CD4+, CD8-, TCR Vα2+, Ly5.1+ adoptively transferred cells. Cells were then processed for single cell RNA sequencing with 10X Genomics 5'v2 and sequenced in house. Cell matrix was created via Cell Ranger and data was processed in Seurat. A) UMAP dimensionality reduction depicting high level clustering. Clustering and UMAP performed in Seurat. B) Dot Plot showing gene expression used for cluster definitions. C) Violin Plot illustrating higher gene expression for *Cxcl10* with similar levels of *Dpp4* expression.

Spectral Flow Cytometry confirms CXCL10 protein expression in T_{FH} and in an overrepresented cluster within the NK replete pool.

In parallel, we are using high-dimensional flow cytometry focused on cell surface markers to delineate the the proteomic features of these transgenic CD4 T cells early after infection in the presence or absence of NK cells.

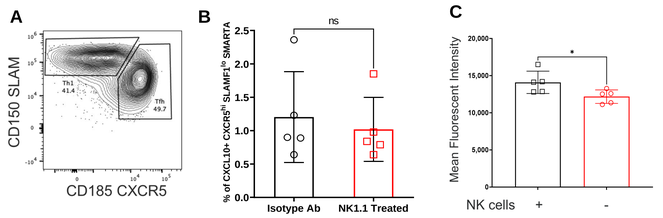

Figure 11. T_{FH} from NK replete animals have more CXCL10 protein. A) Gating strategy for T_{FH} vs Th1 B) Frequency of CXCL10+ T_{FH}. C) Mean Fluorescent intensity for CXCL10 among CXCL10+ cells. (mean±s.e.m.)

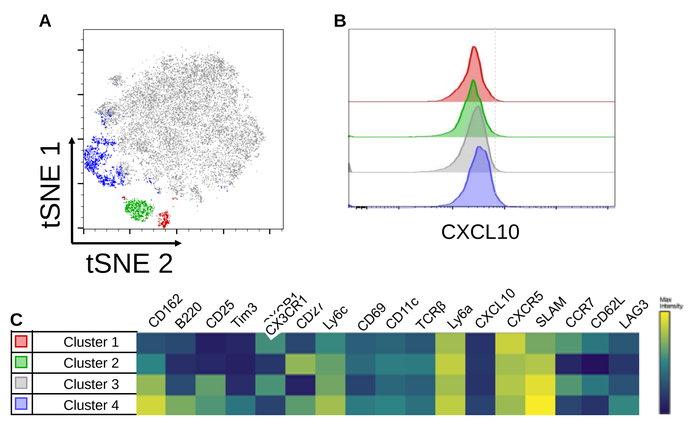

Figure 12. The cluster containing CXCL10+ cells group together with unsupervised clustering and express higher PSGL-1, Ly6c, LAG3 and Tim-3 A) tSNE plot showing X-shift calculated clusters. tSNE and X-shift performed within FlowJo. B) CXCL10 expression by cluster C) Heatmap for protein expression differences between clusters. Calculated by Cluster Explorer within FlowJo

Conclusions

We have developed a model system in that is allowing us to characterize the molecular and proteomic features of the population of T cells that are enriched or eliminated in the presence of NK cells. CXCL10 was enriched in the cell from NK replete animals suggesting that its expression may have a protective effect.

This protective effect may be due to a post translationally modified form of CXCL10 that is cleaved by the peptidase DPP4 (mRNA levels shown in Fig 10 A). DPP4 has been shown to cleave CXCL10 in vitro and in vivo as well as to have negative effects on lymphocyte trafficking. In fact inhibition of DPP4 with sitagliptin increases lymphocyte trafficking and has shown to alter CXCL10 levels in humans[4,5].

Altogether this represent promising preliminary data that will be followed up with additional genetic models wherein CXCL10 and/or DPP4 are knocked out of SMARTA in collaboration with Dr. Schwartzberg at the NIH. Additionally, pharmacologic inhibition will be pursued with the oral sitagliptin which has efficacy in mice.

References and Acknowledgments

1) Rydyznski, C. et al. (2015) Generation of cellular immune memory and B-cell immunity is impaired by natural killer cells. Nat. Commun. 6, 6375 7.

2) Rydyznski, C.E. et al. (2018) Affinity maturation is impaired by natural killer cell suppression of germinal centers. Cell Rep. 24, 3367–3373.

3) Waggoner, S.N. et al (2011) Natural killer cells act as rheostats modulating antiviral T cells. Nature. Nov 20; 481(7241):394-8

4) da Silva, R.B. et al. (2015) Dipeptidylpeptidase 4 inhibition enhances lymphocyte trafficking, improving both naturally occurring tumor immunity and immunotherapy. Nat Immunol. Aug;16(8):850-8

5) Decalf, J. et al. (2016) Inhibition of DPP4 activity in humans establishes its in vivo role in CXCL10 post-translational modification: prospective placebo-controlled clinical studies. EMBO Mol Med Jun; 8(6): 679-83

Work was supported by National Institutes of Health (NIH) grants DA038017, AI148080, AR073228, AI145304. Andrew Cox is supported by NICHD grant K12HD000850 as a Fellow in the Pediatric Scientist Development Program.

We would like to acknowledge the assistance of the Gene Expression Core and the Research Flow Cytometry Core in the Division of Rheumatology at Cincinnati Children's Hospital Medical Center.

All flow cytometric data were acquired using equipment maintained by the Research Flow Cytometry Core in the Division of Rheumatology at Cincinnati Children's Hospital Medical Center supported by NIH S10OD025045. Figures 1 and 6 created with BioRender.